

## Structural and Photophysical Studies of $\text{Cu}(\text{NN})_2^+$ Systems in the Solid State. Emission at Last from Complexes with Simple 1,10-Phenanthroline Ligands

Corey T. Cunningham, Jeffrey J. Moore, Kurstan L. H. Cunningham,  
Phillip E. Fanwick, and David R. McMillin\*

Department of Chemistry, Purdue University, West Lafayette, Indiana 47907-1393

Received January 25, 2000

For a variety of reasons, relating the photophysical properties of a copper phenanthroline to a structure in solution is problematic. To elucidate some of the issues involved, in this paper we describe the crystal and molecular structures of a series of  $\text{Cu}(\text{NN})_2^+$ -containing systems along with spectral data obtained from the solids themselves. The NN ligands investigated are tmp (3,4,7,8-tetramethyl-1,10-phenanthroline), dpdmp (2,9-diphenyl-4,7-dimethyl-1,10-phenanthroline), dptmp (2,9-diphenyl-3,4,7,8-tetramethyl-1,10-phenanthroline), and dipp (2,9-diisopropyl-1,10-phenanthroline). The results show that a flattening distortion can have a large impact on the spectroscopic properties of a  $\text{Cu}(\text{NN})_2^+$  system, whereas a typical rocking distortion has comparatively little effect. The reflectance spectra of orange or orange-red salts that have approximately perpendicular phenanthroline ligands exhibit absorption bands in the neighborhood of 460 nm along with a shoulder at longer wavelength. In the other limit, when a pronounced flattening distortion occurs and the dihedral angle between ligands is  $20^\circ$  or more off perpendicular, the reflectance spectrum exhibits two distinct visible bands with intense absorption occurring at 525 nm or even longer wavelength. If the phenanthroline ligand lacks bulky substituents in the 2,9 positions, the compound may even be purple, depending on the counterion.  $\text{Cu}(\text{NN})_2^+$  complexes that contain phenyl substituents in the 2,9 positions and exhibit long-wavelength absorption in solution probably adopt a flattened structure in the ground electronic state. In most other systems ground-state flattening is a solid-state effect induced by lattice forces. However, a flattening distortion is an intrinsic attribute of the emissive excited state, although intra- or intermolecular forces can inhibit the effect. In the case of the  $\text{Cu}(\text{dptmp})_2^+$  system, intramolecular steric interactions oppose flattening because the methyl groups in the 3,8 positions control the torsion angles of the neighboring phenyl groups. In the case of  $[\text{Cu}(\text{tmp})_2]\text{BPh}_4$ , packing interactions induce a small flattening in the crystal, but they also constrain the degree of distortion that can occur in the excited state. As a consequence  $[\text{Cu}(\text{tmp})_2]\text{BPh}_4$  exhibits a weak photoluminescence in the solid phase ( $\tau = 15$  ns). This is the first report of emission from a bis(phenanthroline)copper(I) system that does not have bulky substituents in the 2 and/or 9 positions of the ligand. The  $[\text{Cu}(\text{tmp})_2]\text{BPh}_4$  system crystallizes in space group  $P2_1/n$  with  $a = 17.4883(4)$  Å,  $b = 9.86860(10)$  Å,  $c = 26.3747(6)$  Å,  $\alpha = 90^\circ$ ,  $\beta = 97.7021(8)^\circ$ ,  $\gamma = 90^\circ$ ,  $V = 4510.8(3)$  Å<sup>3</sup>, and  $Z = 4$ . For 12 948 unique data with  $F_o^2 > 2\sigma(F_o^2)$ ,  $R = 6.5\%$ . The  $[\text{Cu}(\text{dpdmp})_2]\text{PF}_6$  system crystallizes in space group  $P2/n$  with  $a = 16.0722(13)$  Å,  $b = 8.1100(7)$  Å,  $c = 16.8937(10)$  Å,  $\alpha = 90^\circ$ ,  $\beta = 93.947(5)^\circ$ ,  $\gamma = 90^\circ$ ,  $V = 2196.8(5)$  Å<sup>3</sup>, and  $Z = 2$ . For 2833 unique data with  $F_o^2 > 2\sigma(F_o^2)$ ,  $R = 6.0\%$ . The  $[\text{Cu}(\text{dptmp})_2]\text{PF}_6 \cdot \text{THF}$  system crystallizes in space group  $P\bar{1}$  with  $a = 12.8486(4)$  Å,  $b = 13.7341(1)$  Å,  $c = 15.1678(3)$  Å,  $\alpha = 99.5819(14)^\circ$ ,  $\beta = 96.7263(13)^\circ$ ,  $\gamma = 97.3311(12)^\circ$ ,  $V = 2591.3(2)$  Å<sup>3</sup>, and  $Z = 2$ . For 13 753 unique data with  $F_o^2 > 2\sigma(F_o^2)$ ,  $R = 7.4\%$ . Finally, the  $[\text{Cu}(\text{dipp})_2]\text{TfPB}$  system crystallizes in space group  $P\bar{1}$  with  $a = 14.2523(3)$  Å,  $b = 16.0496(4)$  Å,  $c = 17.5801(3)$  Å,  $\alpha = 112.4150(13)^\circ$ ,  $\beta = 105.7480(13)^\circ$ ,  $\gamma = 99.6078(11)^\circ$ ,  $V = 3408.7(3)$  Å<sup>3</sup>, and  $Z = 2$ . For 8774 unique data with  $F_o^2 > 2\sigma(F_o^2)$ ,  $R = 9.3\%$ .

### Introduction

Stereoelectronic effects play extremely important roles in the ground- and excited-state chemistry of bisphenanthroline complexes of copper(I), or  $\text{Cu}(\text{NN})_2^+$  systems for short.<sup>1–3</sup> For example, structure changes play an important role in determining the kinetics and thermodynamics of electron-transfer reactions

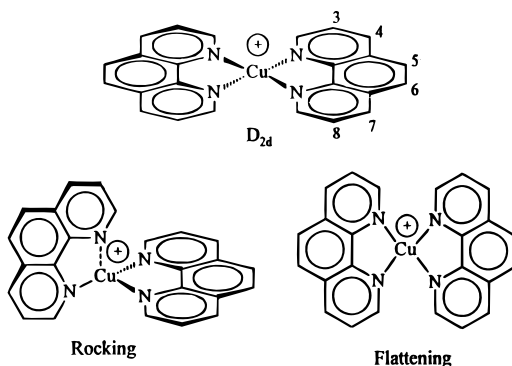
involving the copper center.<sup>1,4a</sup> Sauvage and co-workers recently exploited this effect in an effort to construct a molecular machine in which a photoinduced oxidation reaction triggers linkage isomerization in a copper catenate.<sup>4b</sup> In principle, knowledge of structure is essential for understanding the spectroscopic properties and the reactivity; however, for copper phenanthrolines the structure that occurs in solution is frequently not the one that occurs in a crystal.<sup>5</sup> Indeed, packing-induced, low-symmetry distortions from an idealized pseudotetrahedral

\* To whom correspondence should be addressed. Fax: (765) 494-0239. E-mail: mcmillin@purdue.edu.

- (1) James, B. R.; Williams, R. J. P. *J. Chem. Soc.* **1961**, 2007–2019.
- (2) (a) McMillin, D. R.; McNett, K. M. *Chem. Rev.* **1998**, *98*, 1201–1219. (b) Tamilarasan, R.; Liu, F.; McMillin, D. R. In *Metal-DNA Chemistry*; Tullius, T. D., Ed.; ACS Symposium Series 402; American Chemical Society: Washington, DC, 1989; pp 48–58.
- (3) Meyer, M.; Albrecht-Gary, A. M.; Dietrich-Buchecker, C. O.; Sauvage, J. P. *Inorg. Chem.* **1999**, *38*, 2279–2287.

- (4) (a) Koshino, N.; Kuchiyama, Y.; Ozaki, H.; Funahashi, S.; Takagi, H. D. *Inorg. Chem.* **1999**, *38*, 3352–3360. (b) Livoreil, A.; Sauvage, J. P.; Armaroli, N.; Balzani, V.; Flamigni, L.; Ventura, B. *J. Am. Chem. Soc.* **1997**, *119*, 12114–12124.
- (5) Goodwin, K. V.; McMillin, D. R.; Robinson, W. R. *Inorg. Chem.* **1986**, *25*, 2033–2036.

Chart 1



geometry are quite common in solids containing  $\text{Cu}(\text{NN})_2^+$  complexes on account of the low coordination number and the  $d^{10}$  electronic configuration at the metal center. Perhaps the most common distortion is a  $D_2$  flattening, and, in line with a lattice effect, the degree of flattening varies with the counterion in structures containing the  $\text{Cu}(\text{dmp})_2^+$  cation<sup>6,7</sup> (dmp = 2,9-dimethyl-1,10-phenanthroline). A “rocking” distortion that results in one long Cu–N bond and a pyramidal coordination geometry can occur as well, especially in phenanthroline complexes with aryl substituents in the 2,9 positions.<sup>8–10</sup> In Chart 1 the middle structure represents idealized  $D_{2d}$  symmetry and also presents the atom-numbering system for the free 1,10-phenanthroline (phen) ligand. In this geometry the dihedral angle between ligands is  $90^\circ$ . The other two structures depict complexes that have undergone rocking (left) or severe flattening (right) distortions. The  $\text{Cu}(\text{dpp})_2^+$  system is notable in this regard because it tends to show both types of distortions in the solid state<sup>9,10</sup> (dpp = 2,9-diphenyl-1,10-phenanthroline). In solution, a  $\text{Cu}(\text{NN})_2^+$  chromophore generally adopts a more regular structure, although emission polarization studies indicate that some degree of a static or dynamic flattening distortion occurs.<sup>11,12</sup> However, the situation is very different in the lowest-energy, thermally equilibrated electronic excited state, a metal-to-ligand charge-transfer (CT) state that formally contains a Jahn–Teller-active copper(II) center.<sup>2,13</sup> Thus, systematic studies of substituent effects<sup>13–16</sup> as well as theoretical calculations<sup>14</sup> reveal that the excited state tends to undergo a pronounced flattening distortion. To inhibit the distortion, one has to introduce bulky substituents in the 2,9 positions of the phenanthroline ligand. Without such steric constraints in place, i.e., in a complex such as  $\text{Cu}(\text{phen})_2^+$ , the flattening is severe, even in a low-temperature glass, and there is no hint of an emission signal due to the efficiency of the radiationless decay process.<sup>13,14</sup>

The approach taken here is to define the crystal and molecular structures of a series of  $\text{Cu}(\text{NN})_2^+$ -containing systems and to carry out spectral studies in the same phase. One of the new insights that comes from this work is that packing forces can cut both ways: Packing forces can induce flattening in the ground state, but they can also constrain the degree of distortion that occurs in the excited state. This effect accounts for the emission from crystalline  $[\text{Cu}(\text{tmp})_2]\text{BPh}_4$ , the first example of a luminescent bisphenanthroline complex of copper(I) that does not have sterically active substituents in the 2 and/or 9 positions of the ligand (tmp = 3,4,7,8-tetramethyl-1,10-phenanthroline and  $\text{BPh}_4^-$  = tetraphenylboronate ion). A comparison of the structures of the complexes of 2,9-diphenyl-3,4,7,8-tetramethyl-1,10-phenanthroline (dptmp) and a dimethyl analogue, 2,9-diphenyl-4,7-dimethyl-1,10-phenanthroline, or dpdmp, illustrates how bulky groups in the 3,8 positions of the phenanthroline ligand can, in conjunction with sterically active substituents in the neighboring 2,9 positions, markedly influence the geometry. The structure of  $[\text{Cu}(\text{dipp})_2]\text{TFPB}$  provides the first example of a system that has branched alkyl groups directly linked to the phenanthroline ligand (dipp = 2,9-diisopropyl-1,10-phenanthroline and  $\text{TFPB}^-$  = tetrakis(3,5-bis(trifluoromethyl)phenyl)boronate ion). Finally, spectral studies establish that an intense long-wavelength absorption band is the most reliable indication of a significant flattening distortion in a solid or in solution.

## Experimental Section

**Materials and Methods.** The phen and tmp ligands and the salts  $\text{KPF}_6$  and  $\text{NaBPh}_4$  were reagent-grade products of Aldrich Chemical Co. Samples of  $[\text{Cu}(\text{dipp})_2]\text{TFPB}$ ,<sup>17</sup>  $[\text{Cu}(\text{dpdmp})_2]\text{PF}_6 \cdot \frac{1}{2}\text{H}_2\text{O}$ ,<sup>16</sup>  $[\text{Cu}(\text{dptmp})_2]\text{PF}_6 \cdot 2\text{H}_2\text{O}$ ,<sup>16</sup> and  $[\text{Cu}(\text{dpp})_2]\text{PF}_6$ <sup>18</sup> were available from previous studies. The method of Ruthkowsky et al.<sup>19</sup> served well for the synthesis of the air-sensitive phen and tmp complexes from the precursor  $[\text{Cu}(\text{NCCCH}_3)_4]\text{PF}_6$ .<sup>20</sup> When anion exchange was necessary, a metathesis reaction with a soluble alkali-metal salt in ethanol/water proved effective. For the solid-state emission measurements the sample container was a melting-point capillary positioned in a finger dewar. A 452 nm notch filter in the excitation beam helped isolate the excitation wavelength of 440 nm, and a 525 nm cutoff filter protected the detector from the excitation beam. The emission and excitation band-pass settings were each 10 nm. During the lifetime measurements, 525 and 575 nm long-wave-pass filters removed stray light from the emission beam. The lifetime estimates ( $\pm 10\%$ ) came from a user-written program which assumed exponential decay.<sup>21</sup> In each case the residual plot justified the use of a single exponential. Measurements on powdered samples dispersed in paraffin oil gave the solid-state reflectance spectra. The sample holder was either a thin piece of coarse paper<sup>22</sup> or a pair of salt plates.

**Instrumentation.** The absorbance data came from a Perkin-Elmer Lambda 4C spectrometer, while an SLM SPF 500C spectrofluorimeter provided the steady-state emission spectra. A description of the apparatus for the lifetime measurements appeared previously.<sup>17</sup> The Nonius KappaCCD package served for the preliminary examination of the crystals and data collection with Mo  $K\alpha$  radiation ( $\lambda = 0.71073 \text{ \AA}$ ). The computer for all structure refinements was an AlphaServer 2100.

- (6) Dobson, J. F.; Green, B. F.; Healy, P. C.; Kennard, C. H. L.; Pakawatchai, C.; White, A. H. *Aust. J. Chem.* **1984**, *37*, 649–659.
- (7) Klemens, F. K.; Fanwick, P. E.; Bibler, J. K.; McMillin, D. R. *Inorg. Chem.* **1989**, *28*, 3076–3079.
- (8) Cesario, M.; Dietrich-Buchecker, C. O.; Guilhem, J.; Pascard, C.; Sauvage, J. P. *J. Chem. Soc., Chem. Commun.* **1985**, 244–247.
- (9) Klemens, F. K.; Palmer, C. E. A.; Rolland, S. M.; Fanwick, P. E.; Sauvage, J. P.; McMillin, D. R. *New J. Chem.* **1990**, *14*, 129–133.
- (10) Miller, M. T.; Gantzel, P. K.; Karpishin, T. B. *Inorg. Chem.* **1998**, *37*, 2285–2290.
- (11) Parker, W. L.; Crosby, G. A. *J. Phys. Chem.* **1989**, *93*, 5692–5696.
- (12) Everly, R. M.; McMillin, D. R. *J. Phys. Chem.* **1991**, *95*, 9071–9075.
- (13) Everly, R. M.; Ziessel, R.; Suffert, J.; McMillin, D. R. *Inorg. Chem.* **1991**, *30*, 559–561.
- (14) Shinozaki, K.; Kaizu, Y. *Bull. Chem. Soc. Jpn.* **1994**, *67*, 2435–2439.
- (15) Eggleston, M. K.; McMillin, D. R.; Koenig, K. S.; Pallenberg, A. J. *Inorg. Chem.* **1997**, *36*, 172–176.
- (16) Cunningham, C. T.; Cunningham, K. L. H.; Michalec, J. F.; McMillin, D. R. *Inorg. Chem.* **1999**, *38*, 4388–4392.

- (17) Cunningham, K. L. H.; McMillin, D. R. *Inorg. Chem.* **1998**, *37*, 4114–4119.
- (18) Everly, R. M.; McMillin, D. R. *Photochem. Photobiol.* **1989**, *50*, 711–716.
- (19) Ruthkowsky, M.; Castellano, F. N.; Meyer, G. J. *Inorg. Chem.* **1996**, *35*, 6406–6412.
- (20) Kubas, G. J. *Inorg. Synth.* **1979**, *19*, 90–91.
- (21) Palmer, C. E. A.; McMillin, D. R.; Kirmaier, C.; Holten, D. *Inorg. Chem.* **1987**, *29*, 3167–3170.
- (22) Shibata, K. In *Methods of Biochemical Analysis*; Glick, D., Ed.; Interscience: New York, 1959; Vol. 7, pp 77–109.

**Table 1.** Crystallographic Data

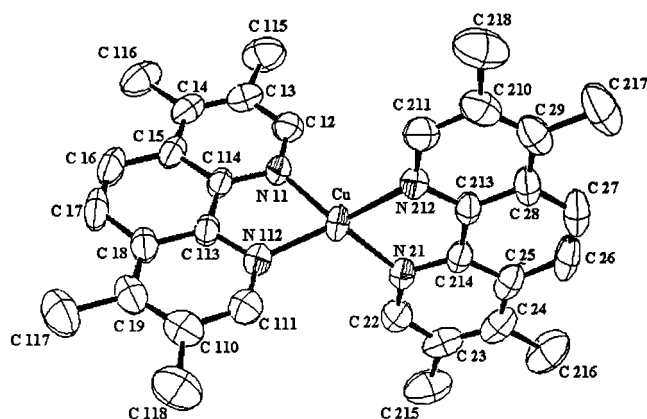
	[Cu(tmp) <sub>2</sub> ]BPh <sub>4</sub>	[Cu(dpdpmp) <sub>2</sub> ]PF <sub>6</sub>	[Cu(dptmp) <sub>2</sub> ]PF <sub>6</sub> ·THF	[Cu(dipp) <sub>2</sub> ]TFPB
empirical formula	CuN <sub>4</sub> C <sub>56</sub> BH <sub>52</sub>	CuC <sub>52</sub> H <sub>40</sub> F <sub>6</sub> N <sub>4</sub> P	CuPF <sub>6</sub> ON <sub>4</sub> C <sub>60</sub> H <sub>56</sub>	CuF <sub>24</sub> N <sub>4</sub> C <sub>68</sub> BH <sub>52</sub>
fw	855.42	929.43	1057.65	1455.51
space group	<i>P</i> 2 <sub>1</sub> / <i>n</i>	<i>P</i> 2/ <i>n</i>	<i>P</i> 1	<i>P</i> 1
<i>a</i> , Å	17.4883(4)	16.0722(13)	12.8486(4)	14.2523(3)
<i>b</i> , Å	9.86860(10)	8.1100(7)	13.7341(4)	16.0496(4)
<i>c</i> , Å	26.3747(6)	16.8937(10)	15.1678(3)	17.5801(3)
α, deg	90	90	99.5819(14)	112.4150(13)
β, deg	97.7021(8)	93.947(5)	96.7263(13)	105.7480(13)
γ, deg	90	90	97.3311(12)	99.6078(11)
<i>V</i> , Å <sup>3</sup>	4510.8(3)	2196.8(5)	2591.3(2)	3408.7(3)
<i>Z</i>	4	2	2	2
temp (K)	296	296	296	296
linear abs coeff, mm <sup>-1</sup>	0.525	0.598	0.516	0.425
transmission coeff	0.770–0.949	0.799–0.956	0.751–0.911	0.706–0.958
λ, Å	0.710 73	0.710 73	0.710 73	0.710 73
GOF	1.031	1.067	1.033	1.031
ρ <sub>calcd</sub> , cm <sup>-3</sup>	1.26	1.405	1.355	1.418
<i>R</i> ( <i>F</i> <sub>o</sub> ), <sup>a</sup> <i>R</i> <sub>w</sub> ( <i>F</i> <sub>o</sub> <sup>2</sup> ) <sup>b</sup>	0.065, 0.157	0.060, 0.139	0.074, 0.190	0.093, 0.253

$$^a R = \sum ||F_o| - |F_c|| / \sum |F_o| \text{ for } F_o^2 > 2\sigma(F_o^2). \quad ^b R_w = [\sum w(|F_o^2| - |F_c^2|)^2 / \sum w|F_o^2|]^2$$

**Crystal Structure Determination.** Vapor diffusion of toluene into a dichloromethane solution of [Cu(tmp)<sub>2</sub>]BPh<sub>4</sub> produced an orange plate of dimensions 0.30 × 0.18 × 0.10 mm that was suitable for diffraction studies. Least-squares refinement of the setting angles of 57 010 reflections in the range 2° < θ < 32° provided cell constants and an orientation matrix for the crystal mounted on a glass fiber. The maximum value of 2θ was 66.0°. The data set contained 12 948 unique reflections, and the average transmission coefficient was 0.905. In each case, for the refinement the input intensity was the average of equivalent reflections (agreement factor 8.8%). The refinement took account of each of the unique reflections, but for this and the refinements that follow only data points that satisfied the criterion  $F_o^2 > 2\sigma(F_o^2)$  affected the calculation of the *R* value. Program PATTY in DIRDIF92<sup>23</sup> gave the solution to the structure, although difference Fourier syntheses were useful for locating some of the atoms. The refinement included hydrogen atoms with the constraint that they ride on the bonded atoms. Table 1 contains cell parameters and refinement data for this and the other structures reported.

Slow diffusion of diethyl ether into an underlying layer of dichloromethane containing [Cu(dpdpmp)<sub>2</sub>]PF<sub>6</sub> yielded a red plate of dimensions 0.40 × 0.28 × 0.08 mm. Least-squares refinement of the setting angles of 12 590 reflections in the range of 4° < θ < 25° gave cell constants and an orientation matrix for the crystal mounted as above. The maximum value of 2θ was 50.1°. There were 2833 unique reflections in the data set, and the average transmission coefficient was 0.910. The input for the refinement was the average of all equivalent reflections (agreement factor of 9.2% on an intensity basis). Direct methods in conjunction with the program SIR97<sup>24</sup> located most of the atoms, and the rest were evident from difference Fourier syntheses. The refinement with the program SHELX-97 included hydrogen atoms constrained to ride on the bonded atoms. The thermal parameters revealed a disorder in the position of the anion as is frequently the case with hexafluorophosphate derivatives. However, there was no attempt to model the disorder since that would entail arbitrary assumptions, and the structure of the cation is the focus of the study.

Vapor diffusion of toluene into a THF solution of [Cu(dptmp)<sub>2</sub>]PF<sub>6</sub>·2H<sub>2</sub>O produced an orange chunk of a monosolvate with dimensions 0.25 × 0.20 × 0.18 mm. Least-squares refinement of the setting angles of 33 837 reflections in the range 3° < θ < 31° (2θ maximum 63.9°) gave cell constants and an orientation matrix for the crystal. In all there were 13 753 unique reflections, and the average transmission coefficient was 0.875. The agreement factor for averaging equivalent intensities

**Figure 1.** ORTEP drawing of the cation in [Cu(tmp)<sub>2</sub>]BPh<sub>4</sub> with 50% thermal ellipsoids and the atom-numbering scheme.

was 5.5%, and the refinement procedure was the one employed for the tmp structure. In this case there was disorder in the positions of the anion as well as the THF of crystallization; however, neither effect has a significant impact on conclusions concerning the structure of the cation.

Slow evaporation of an aqueous ethanol solution of [Cu(dipp)<sub>2</sub>]TFPB yielded a yellow-orange plate with dimensions 0.25 × 0.22 × 0.10 mm for the diffraction study. Least-squares refinement of the setting angles of 43 343 reflections in the range 4° < θ < 30° (2θ maximum 61.0°) gave cell constants and an orientation matrix for the crystal. In all there were 8774 unique reflections, and the average transmission coefficient was 0.894. The agreement factor for averaging equivalent intensities was 6.2%. A direct method using the program SIR97 yielded the solution to the structure. Again, there was evidence of disorder in the positioning of the anion.

## Results

**Crystal Structure of [Cu(tmp)<sub>2</sub>]BPh<sub>4</sub>.** The lattice consists of molecular ions; see Figure 1 for a view of the cation and the atom-numbering scheme, which is the same for the structures described below. Table 2 provides a summary of important interatomic distances and angles for this system and the other structures reported. In essence, the coordination geometry about copper in Cu(tmp)<sub>2</sub><sup>+</sup> is flattened tetrahedral with a dihedral angle (θ<sub>2</sub>) of 98.2(1)° between the Cu–N(11)–N(112) and Cu–N(21)–N(212) planes. In the crystal, copper complexes mesh together into chains running along the *b* axis. Each chain involves two stacks of ligands. Down each stack, ligand 1 of one complex faces against ligand 2 of the next neighbor which

(23) Beurskens, G.; Admirall, G.; Beurskens, G.; Bosman, W. P.; Garcia-Granda, S.; Gould, R. O.; Smits, J. M. M.; Smykalla, C. *The DIRDIF92 Program System*; Technical Report; Crystallography Laboratory, University of Nijmegen: Nijmegen, The Netherlands, 1992.

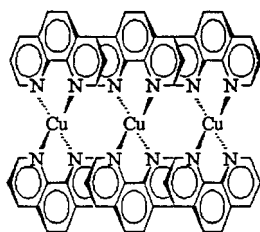
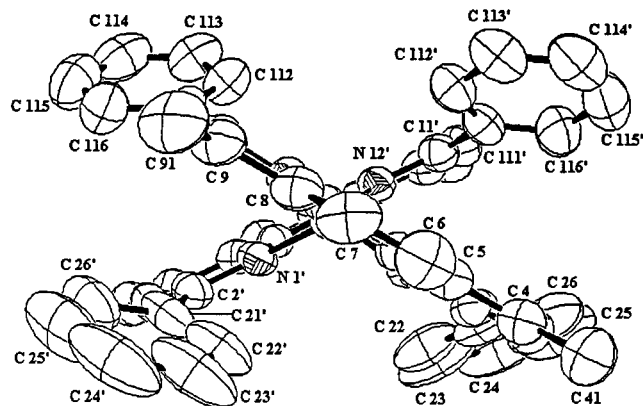
(24) Altomare, A.; Cascarano, G.; Giacovazzo, C.; Guagliardi, A.; Moliterni, A. G. G.; Burla, M. C.; Polidori, G.; Camalli, M.; Spagna, R. *J. Appl. Crystallogr.* **1999**, *32*, 115–119.



**Table 2.** Selected Structural Data<sup>a</sup>

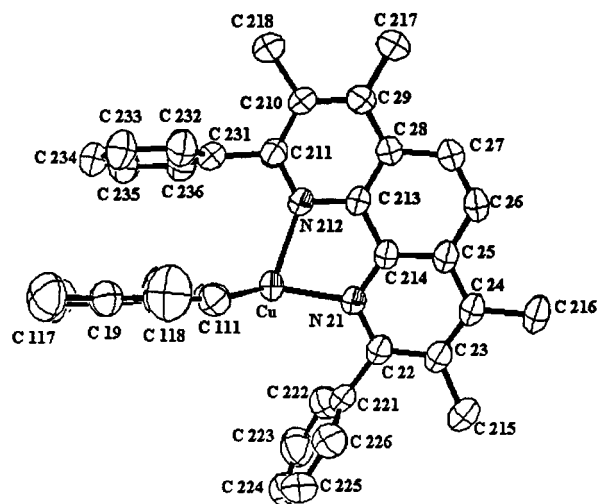
	$[\text{Cu}(\text{tmp})_2]\text{BPh}_4$	$[\text{Cu}(\text{dpdmp})_2]\text{PF}_6$	$[\text{Cu}(\text{dptmp})_2]\text{PF}_6 \cdot \text{THF}$	$[\text{Cu}(\text{dipp})_2]\text{TFPB}$
Cu–N(11) (Å)	2.053(2)	2.042(3)	2.058(3)	2.068(5)
Cu–N(112) (Å)	2.034(2)	2.042(3)	2.039(3)	2.007(5)
Cu–N(21) (Å)	2.039(2)	2.053(3)	1.993(3)	2.053(5)
Cu–N(212) (Å)	2.048(2)	2.053(3)	2.150(3)	2.020(5)
N(112)–Cu–N(21) (deg)	122.94(10)	114.21(13)	128.85(12)	122.6(2)
N(112)–Cu–N(212) (deg)	132.49(9)	134.7(2)	108.22(11)	132.8(2)
N(21)–Cu–N(212) (deg)	81.29(9)	81.97(13)	81.23(11)	82.76(19)
N(112)–Cu–N(11) (deg)	81.20(9)	81.97(13)	81.82(11)	82.6(2)
N(21)–Cu–N(11) (deg)	126.49(9)	138.90(19)	140.15(12)	117.60(19)
N(212)–Cu–N(11) (deg)	118.95(9)	114.21(13)	116.18(11)	123.09(19)
$\theta_x^b$ (deg)	88.8	92.1	108.9	93.3
$\theta_y^b$ (deg)	85.9	91.5	97.8	83.9
$\theta_z^b$ (deg)	98.2	68.4	87.9	88.2

<sup>a</sup> For the dpdmp complex the numbering scheme differs as follows N(11)=N(1), N(112)=N(12), N(21)=N(1)', N(212)=N(12)'. <sup>b</sup>  $\theta_x$  is the angle between the bisector ( $\xi$ ) of the N(21)–Cu–N(212) angle and the normal to the N(11)–Cu–N(112) plane (P1).  $\theta_y$  is the angle between  $\xi$  and the normal to the bisector of the N(11)–Cu–N(112) angle in P1 on the N(11) side. Finally,  $\theta_z$  is the angle between the normals to P1 and P2 (the N(21)–Cu–N(212) plane).<sup>6</sup>

**Figure 2.** Schematic view of a meshed chain of  $\text{Cu}(\text{tmp})_2^+$  ions in the lattice with the Cu–Cu vectors along the  $b$  axis.**Figure 3.** ORTEP view through the phenanthroline ligands of the copper complex in  $[\text{Cu}(\text{dpdpmp})_2]\text{PF}_6$ . The view is normal to the axis of flattening, which is collinear with the vertical  $C_2$  symmetry axis.

faces upon ligand 1 of the next complex and so on in the sequence (Figure 2). The orientation is such that the short axis of each phenanthroline moiety is roughly parallel to the  $a$  axis of the crystal. The only atom–atom contacts of less than 3.5 Å are N(21)–C(111) at 3.436 (4) Å, C(22)–N(112) at 3.403 (4) Å, and C(22)–N(111) at 3.410 (4) Å.

**Crystal Structure of  $[\text{Cu}(\text{dpdmp})_2]\text{PF}_6$ .** Figure 3 provides a view of the  $\text{Cu}(\text{dpdmp})_2^+$  complex, which exhibits a more pronounced flattening distortion in the crystal with  $\theta_z = 68.4(1)^\circ$ . A  $C_2$  axis, vertically oriented in Figure 3, passes through the copper atom and interconverts the two ligands. There are no significant interligand contacts between neighbor complexes in the structure, and the least-squares planes defined by the C(2N) and C(11N) phenyls subtend dihedral angles of 44.74(14)° and 134.84(16)°, respectively, relative to the mean plane of the phenanthroline core. (Here and in the following,  $N$  ranges from 1 to 6 in the atom-numbering system for the phenyl substituents.)

**Figure 4.** ORTEP view and atom numbering of the cation in  $[\text{Cu}(\text{dptmp})_2]\text{PF}_6 \cdot \text{THF}$  with the C(12N) and C(13N) phenyls removed for clarity. The view is in the plane of ligand 1, and the elongated N(212)–Cu bond defines the apex of the approximate trigonal pyramid around copper. Phenyl C(23N) stacks on ligand 1. The C(12N) phenyl would be in the foreground attached to C12.

**Crystal Structure of  $[\text{Cu}(\text{dptmp})_2]\text{PF}_6 \cdot \text{THF}$ .** Figure 4 provides a view of the dptmp complex. In this structure the convention is that the C(22N) phenyl connects to C(22), but for convenience in numbering the C(23N) phenyl connects to C(211). The methyl carbons are C(215)–C(218), and analogous conventions apply to the numbering for ligand 1. (For clarity Figure 4 does not show the C(12N) and C(13N) phenyls, which would be in the foreground and background, respectively, of ligand 2.) In contrast to the dpdmp analogue, the dptmp complex exhibits little flattening as  $\theta_z = 87.9(1)^\circ$ . However, a significant rocking distortion produces an exceptionally long Cu–N(212) bond length (Table 2) and an approximately trigonal pyramidal coordination geometry at copper. The distortion facilitates the stacking of the C(23N) phenyl group on the opposite phenanthroline ligand, i.e., ligand 1, such that the angle between the least-squares planes of the two groups is 6.63(69)°. On the other hand, the C(22N) and C(23N) phenyl rings are more nearly orthogonal to the parent phenanthroline core as they subtend dihedral angles of 103.65(13)° and 99.42(11)°, respectively. The corresponding twist angles of the C(12N) and C(13N) phenyls are 128.09(13)° and 77.34(18)°, respectively, and the sense of the twists is disrotatory to create space for the C(22N) phenyl group. Intermolecular interactions occur as well as the copper

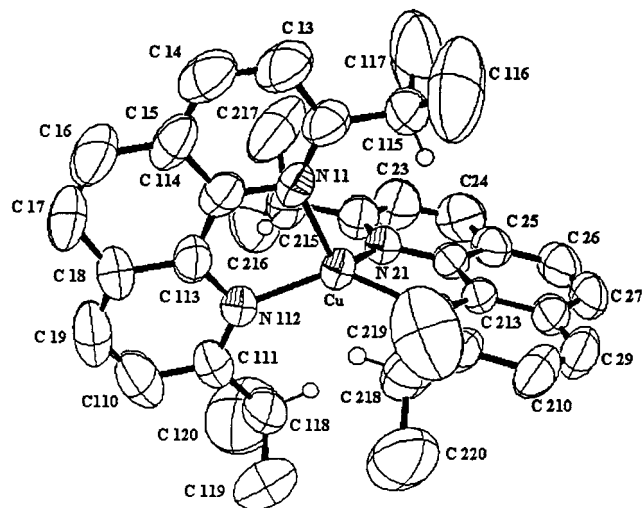


**Figure 5.** ORTEP drawing and atom numbering of the cation in  $[\text{Cu}(\text{dipp})_2]\text{TFPB}$  with 50% thermal ellipsoids.

complexes associate as dimers with the back edge of ligand 1 from one member of the pair partially stacked over ligand 1 of the partner. Close contacts include  $\text{C}(14)\text{--}\text{C}(18)$  at 3.53(6) Å and  $\text{C}(16)\text{--}\text{C}(114)$  at 3.38(6) Å.

**Crystal Structure of  $[\text{Cu}(\text{dipp})_2]\text{TFPB}$ .** Figure 5 provides a view of  $\text{Cu}(\text{dipp})_2^+$ . In large part because of the presence of the TFPB anion, the quality of this structure is poor in comparison to the others as the thermal parameters reveal considerable static or thermal disorder in the positions of the various  $\text{CF}_3$  groups. As a consequence one cannot press the interpretation too far; nevertheless, the structure provides some useful information. Thus, with  $\theta_z = 88.8(2)^\circ$ , the copper complex shows no significant flattening in the solid state. Although Table 1 shows that the variations in the  $\text{Cu}\text{--}\text{N}$  bond lengths in the complex are modest, ligand 1 may show a small rocking displacement, with the  $\text{Cu}\text{--}\text{N}(11)$  bond about 0.06 Å longer than that of  $\text{Cu}\text{--}\text{N}(112)$ . However, the thermal ellipsoids in Figure 5 suggest that movement along the rocking coordinate is relatively facile in the lattice. Throughout the lattice the  $\text{Cu}(\text{dipp})_2^+$  complexes distribute as weakly interacting dimers related by a center of inversion. However, the interligand overlap is small, and the interatomic distances are too great for a significant stacking interaction. Therefore, intramolecular forces must determine the coordination geometry, which, of the four structures reported herein, comes the closest to  $D_{2d}$  symmetry. The steric bulk associated with the isopropyl groups is undoubtedly the key consideration. Although the thermal ellipsoids associated with the methyl carbons are also large (Figure 5), on average the methyl–methyl vector of each isopropyl substituent orients in a direction roughly orthogonal to the mean plane of the phenanthroline core, with the  $\text{C}\text{--}\text{H}$  bond of the  $\alpha$ -carbon extending toward the other ligand bound to copper. The steric demands of the substituents account for the previous observation that the photoexcited state of  $\text{Cu}(\text{dipp})_2^+$  undergoes unusually facile electron-transfer quenching.<sup>17</sup> Thus, with intramolecular steric forces constraining the geometry, formation of the excited state entails minimal structural reorganization.

**Absorption and Emission Studies.** The solid-state reflectance spectra of the  $[\text{Cu}(\text{NN})_2]\text{X}$  systems investigated to date fall into one of two limiting types; however, for any given NN ligand the spectrum may vary with the nature of the anion  $\text{X}^-$ . With a broad maximum at around 440 nm and a shoulder at ca. 520 nm, the reflectance spectrum of the orange compound  $[\text{Cu}(\text{tmp})_2]\text{BPh}_4$  is an example of the class I type (Figure 6B). The

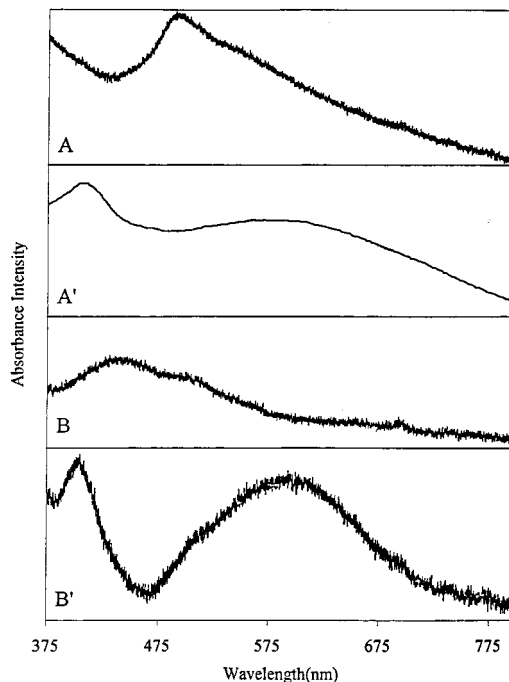


**Figure 6.** Reflectance spectra: (A)  $[\text{Cu}(\text{phen})_2]\text{BPh}_4$ , (A')  $[\text{Cu}(\text{phen})_2]\text{ClO}_4$ ,<sup>14</sup> (B)  $[\text{Cu}(\text{tmp})_2]\text{BPh}_4$ , (B')  $[\text{Cu}(\text{tmp})_2]\text{PF}_6$ . Absolute intensities are arbitrary.

**Table 3.** Room-Temperature Spectral Data for the Solid State

compound	reflectance		emission <sup>a</sup>	
	$\lambda_{\text{max}}$ , nm	$\lambda_{\text{max}}$ , nm	$\lambda_{\text{max}}$ , nm	$\tau$ , ns
Class I Spectra				
$[\text{Cu}(\text{tmp})_2]\text{BPh}_4$	440 (505 sh)	700	15	
$[\text{Cu}(\text{phen})_2]\text{BPh}_4$	485 (545 sh)	690	20	
$[\text{Cu}(\text{dipp})_2]\text{TFPB}$	465 (530 sh)	630	1330	
$[\text{Cu}(\text{dptmp})_2]\text{PF}_6 \cdot \text{THF}$	485	655	1570	
Intermediate				
$[\text{Cu}(\text{dpp})_2]\text{PF}_6^b$	500 (560 sh)	670	780	
Class II Spectra				
$[\text{Cu}(\text{tmp})_2]\text{PF}_6$	405 595			
$[\text{Cu}(\text{phen})_2]\text{ClO}_4^c$	410 580			
$[\text{Cu}(\text{dpdmp})_2]\text{PF}_6$	420 535	685	325	

<sup>a</sup> Uncorrected. <sup>b</sup> Broad absorption. <sup>c</sup> Reference 14.

spectrum of  $[\text{Cu}(\text{phen})_2]\text{BPh}_4$  has the same profile with its maximum around 480 nm and a shoulder at 550 nm (Figure 6A). In contrast, the purple compounds  $[\text{Cu}(\text{tmp})_2]\text{PF}_6$  (Figure 6B') and  $[\text{Cu}(\text{phen})_2]\text{ClO}_4$  (Figure 6A') exhibit prototypical reflectance spectra of the class II type for which a second absorbance maximum occurs at a significantly longer wavelength, typically beyond 525 nm. The solid-state data compiled in Table 3 show that  $[\text{Cu}(\text{dipp})_2]\text{TFPB}$  also gives a class I reflectance spectrum. Table 3 also includes results from a series of systems with phenyl substituents in the 2,9 positions of the phenanthroline ligand. The spectrum of  $[\text{Cu}(\text{dptmp})_2]\text{PF}_6 \cdot \text{THF}$  is consistent with class I behavior, but  $[\text{Cu}(\text{dpdmp})_2]\text{PF}_6$  clearly exhibits a class II spectrum with a broad absorbance centered around 535 nm and another maximum at ca. 420 nm.

All four structurally characterized complexes exhibit broad featureless emission spectra (data summary in Table 3). Figure 7 includes the solid-state emission spectra of  $[\text{Cu}(\text{phen})_2]\text{BPh}_4$  and  $[\text{Cu}(\text{tmp})_2]\text{BPh}_4$  as well as other relevant compounds and provides an indication of the relative emission intensities for the series. (The sample configuration and the instrumental gain setting were the same for each compound; however, the quantitative comparison assumes that each solid has the same

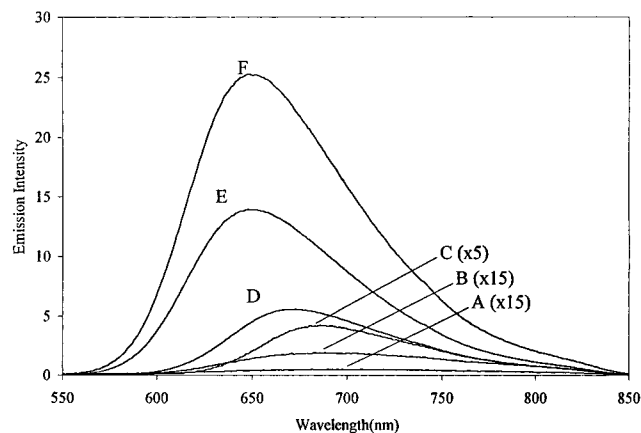


**Figure 7.** Room-temperature, uncorrected emission spectra of  $\text{Cu}(\text{NN})_2^+$  centers in different solids: (A)  $[\text{Cu}(\text{tmp})_2]\text{BPh}_4$ , (B)  $[\text{Cu}(\text{phen})_2]\text{BPh}_4$ , (C)  $[\text{Cu}(\text{dpdmp})_2]\text{PF}_6$ , (D)  $[\text{Cu}(\text{dpp})_2]\text{PF}_6$ , (E)  $[\text{Cu}(\text{dptmp})_2]\text{PF}_6$ , (F)  $[\text{Cu}(\text{dipp})_2]\text{TfPB}$ . All are referenced to the same instrumental gain setting.

absorption cross section at the exciting wavelength.) Note that the short-lived emissions from  $[\text{Cu}(\text{phen})_2]\text{BPh}_4$  and  $[\text{Cu}(\text{tmp})_2]\text{BPh}_4$  occur at relatively long wavelengths (Table 3).

## Discussion

**Ground-State Distortions.** The copper complexes in  $[\text{Cu}(\text{tmp})_2]\text{BPh}_4$  and  $[\text{Cu}(\text{dpdmp})_2]\text{PF}_6$  both exhibit  $D_2$ -flattening distortions in the solid state, but the forces that control the geometry are not easy to identify. Dobson et al. originally attributed the distortions to packing forces,<sup>6</sup> and Goodwin et al. subsequently proposed that stacking interactions between ligands on adjacent metal centers mediated the effect.<sup>5</sup> However, intermolecular stacking interactions are at best one factor because in this study the most flattened  $\text{Cu}(\text{NN})_2^+$  unit occurs in  $[\text{Cu}(\text{dpdmp})_2]\text{PF}_6$ , where there is no stacking. Goodwin et al. also noted that the ionic size would have an effect on the Coulombic forces in the lattice,<sup>5</sup> and the hope of reducing this interaction was one of the motivating factors for including  $[\text{Cu}(\text{tmp})_2]\text{BPh}_4$  in the present investigation. In fact, the dihedral angle between ligands turns out to be much greater in  $[\text{Cu}(\text{tmp})_2]\text{BPh}_4$  ( $98.2^\circ$ ) with its larger cation and anion than in  $[\text{Cu}(\text{phen})_2]\text{ClO}_4$  ( $49.9^\circ$ ).<sup>25</sup> However, no clear, across-the-board trend emerges because the flattening distortion is greater in  $[\text{Cu}(\text{dpdmp})_2]\text{PF}_6$  than in  $[\text{Cu}(\text{dpp})_2]\text{PF}_6$ , even though the dpp derivative involves an ostensibly smaller cation. The fact is that the size of the cation is a rather nebulous concept because the ions can interpenetrate each other and because the coordination geometry of the  $\text{Cu}(\text{NN})_2^+$  center varies with the anion.

As noted above,  $\text{Cu}(\text{NN})_2^+$  complexes with aryl substituents in the 2,9 positions frequently exhibit a rocking distortion that gives rise to a pyramidal coordination geometry in addition to a flattening distortion. Sauvage and co-workers first described the rocking distortion in the catenate  $\text{Cu}(\text{cat}-30)^+$ .<sup>8</sup> Later work revealed that similar distortions occur in  $[\text{Cu}(\text{dpp})_2]\text{CuCl}_2 \cdot \frac{2}{3}\text{CH}_3\text{CN}$ <sup>9</sup> and  $[\text{Cu}(\text{dpp})_2]\text{PF}_6$ .<sup>10</sup> Sauvage and co-workers proposed that the rocking distortion is the result of intra- and intermolecular stacking interactions that occur in the solid state.<sup>8</sup> In fact, the same type of packing interactions occur in  $[\text{Cu}(\text{dptmp})_2]\text{PF}_6 \cdot \text{THF}$ . However, the structure of  $[\text{Cu}(\text{dpdmp})_2]\text{PF}_6$  demonstrates that the presence of the aryl substituents does not guarantee that there will be a rocking distortion. One of the

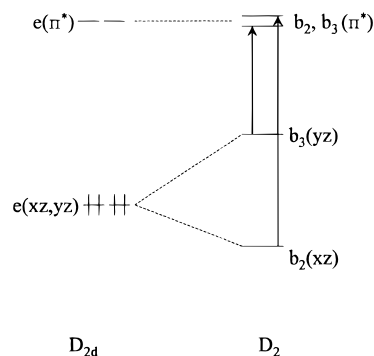


**Figure 8.** Energy-level diagram that shows the effect of a  $D_2$ -flattening distortion on the levels involved in the MLCT transitions of a  $\text{Cu}(\text{NN})_2^+$  center. The scheme assumes that the flattening occurs along the  $x$ -axis and that the  $z$ -axis connects the ligand centers.

intriguing aspects of the dptmp complex is the absence of a flattening distortion due to a cooperative interaction between neighboring substituents. To see how this occurs, focus on the  $D_{2d}$  structure where the phenyl substituents in the 2,9 positions of the phenanthroline ligand define a torsion angle of  $90^\circ$ . A flattening distortion requires that the phenyl groups twist toward the plane of the parent phenanthroline to avoid steric contacts with the opposing ligand. However, with the dptmp ligand, the buttressing 3,8 methyl substituents constrain the motion of the adjacent phenyl groups and favor the retention of a  $90^\circ$  torsion angle. The same effect restricts the distortion in the excited state and enhances the energy and the lifetime of the emission from the dptmp complex in solution.<sup>16</sup>

**Spectral Consequences of Structural Distortions.** The data show that a flattening distortion, as opposed to a rocking distortion, has a big impact on the reflectance spectrum. The results are consistent with the previous studies of Shinozaki and Kaizu on  $[\text{Cu}(\text{phen})_2]\text{ClO}_4$ ,<sup>14</sup> wherein the copper center exhibits a pronounced  $D_2$  distortion and the CT absorption occurs at long wavelengths. The rationalization for the low-energy absorption is apparent in the orbital energy diagram in Figure 8, which assumes that the highest occupied molecular orbitals (HOMOs) of the ground state are a pair of degenerate orbitals with mainly  $d_{xz}$  and  $d_{yz}$  character.<sup>26,27</sup> (In contrast to other references, the calculations of Shinozaki and Kaizu place the  $d_{x^2-y^2}$  orbital as the HOMO,<sup>14</sup> but this does not affect the basic argument because the majority of the oscillator strength involves the  $e_{xz,yz}$  set in any event.<sup>28</sup>) When the flattening occurs along the  $x$ -axis, Figure 8 shows that the  $d_{yz}$  orbital moves to higher energy because of  $\sigma$ -antibonding interactions with the ligand donor orbitals. As the dihedral angle deviates from  $90^\circ$ , a transition from  $d_{yz}$  becomes  $z$ -polarized and allowed by the electric-dipole mechanism,<sup>11,12</sup> until the limit of  $D_{4h}$  symmetry where  $d_{yz}$  finally becomes orthogonal to the  $\pi$ -acceptor orbitals of the ligands. An important practical consideration is that, particularly for systems lacking sterically active ligands, the color can vary from salt to salt. The reason is that a change of counterion can induce a change in the crystal packing and, in turn, in the structure of the absorbing species,  $\text{Cu}(\text{NN})_2^+$ .

A flattening distortion will also lower the emission energy, and the geometry change tends to be even more pronounced in the CT excited state.<sup>13</sup> From one point of view, the effect is evident from the  $e^3$  configuration at copper in the  $D_{2d}$  excited

(26) Daul, C.; Schlapfer, C. W.; Goursot, A.; Penigault, E.; Weber, J. *Chem. Phys. Lett.* **1981**, *78*, 304–310.

(27) Sakaki, S.; Mizutani, H.; Kase, Y. *Inorg. Chem.* **1992**, *31*, 4575–4581.

(28) Phifer, C. C.; McMillin, D. R. *Inorg. Chem.* **1986**, *25*, 1329–1333.

(25) Healy, P. C.; Engelhardt, L. M.; Patrick, J. A.; White, A. H. *J. Chem. Soc., Dalton Trans.* **1985**, 2541–2545.



state, where, in keeping with the copper(II) character, the excited state is subject to a Jahn–Teller distortion. In the context of the state symmetry, the argument is a little more complex. Consider the singlet manifold wherein the  $e^3e^1$  excited-state configuration gives rise to  $^1A_1$ ,  $^1B_1$ ,  $^1B_2$ , and  $^1A_2$  terms. In idealized  $D_{2d}$  symmetry, a  $b_1$  vibration induces a vibronic mixing of  $^1B_2$  and  $^1A_2$  terms and thereby promotes a  $D_2$  distortion. The distortion can be quite significant because in the  $D_2$  point group the motion is totally symmetric and the  $^1B_2(D_{2d})$  and  $^1A_2(D_{2d})$  states become  $^1B_1(D_2)$  states. As Pearson has pointed out, this allows the two states to continue to mix in the lower-symmetry environment, so that a strong second-order Jahn–Teller effect drives down the energy of a  $^1B_1(D_2)$  excited state.<sup>29</sup> Another second-order Jahn–Teller interaction is also possible in  $D_2$  symmetry—hybridization of the  $4s$  and  $3d_{3x^2-r^2}$ , or  $3d_x^2$  for short, orbitals of the copper center, both of which have  $a_1$  symmetry in the  $D_2$  point group. As a consequence, further flattening can take place in the excited state even if the ground state has a flattened ( $D_2$ ) geometry to begin with.

In the absence of a restoring force, the distortion can be so large that the excited-state potential energy surface impinges upon or even crosses that of the ground state, a scenario that virtually guarantees efficient radiationless decay.<sup>30</sup> Consequently, the excited state of a system such as  $\text{Cu}(\text{phen})_2^+$  or  $\text{Cu}(\text{tmp})_2^+$ , which lacks bulky groups in the 2,9 positions of the phenanthroline ligands, is especially prone to a large flattening distortion. For this reason, no one has reported observing photoluminescence from such unhindered systems in solution or even a low-temperature glass.<sup>13,14</sup> Indeed, the emissions observed from the solids  $[\text{Cu}(\text{tmp})_2]\text{BPh}_4$  and  $[\text{Cu}(\text{phen})_2]\text{BPh}_4$  are the first examples of emission from a  $\text{Cu}(\text{NN})_2^+$  system of this type. In the solid state, packing interactions evidently limit the degree of geometric relaxation that can occur in the excited state so that the emission process becomes competitive. Nevertheless, some geometry changes occur in the emitting states because  $[\text{Cu}(\text{phen})_2]\text{BPh}_4$  and  $[\text{Cu}(\text{tmp})_2]\text{BPh}_4$  both emit at longer wavelengths than the  $\text{Cu}(\text{dmp})_2^+$  complex (Figure 7). The trend is quite remarkable in view of the reflectance data and the fact that the introduction of phenyl substituents normally lowers the energy of the emission.<sup>31,32,33</sup>

**Structure in Solution.** Since lattice forces are often responsible for low-symmetry distortions, any particular  $\text{Cu}(\text{NN})_2^+$  chromophore may adopt a different structure in solution.<sup>5</sup> Indeed,  $\text{Cu}(\text{phen})_2^+$  exhibits a very different absorption spectrum in solution as compared with the solid perchlorate salt,<sup>14</sup> and Eggleston et al. have reported a similar effect involving the  $\text{Cu}(\text{dnpp})_2^+$  system (dnpp = 2,9-dineopentyl-1,10-phenanthroline).<sup>34</sup> In both instances cited, the  $\text{Cu}(\text{NN})_2^+$  center adopts a more regular pseudotetrahedral structure in solution according to spectral results.

The  $\text{Cu}(\text{dpp})_2^+$  system is different in that in solution it gives a long-wavelength absorption that is characteristic of a distinctly flattened structure. In fact, the reflectance spectrum of  $[\text{Cu}(\text{dpp})_2]\text{BPh}_4$ , which exhibits a more flattened  $\text{Cu}(\text{NN})_2^+$  center than  $[\text{Cu}(\text{dmp})_2]\text{PF}_6$ , gives a good match to the solution spectrum.<sup>35</sup> Intramolecular forces must be responsible for any distortion that occurs in solution, and Sauvage and co-workers have argued that interligand stacking interactions involving aryl substituents in the 2,9 positions promote a distortion from  $D_{2d}$  symmetry.<sup>3,8</sup> When, as in their systems, the substituents are electron-rich aryl ethers, face-to-face donor–acceptor interactions with the opposite phenanthroline ligand are certainly possible. Intraligand, mesomeric interactions are also potentially important factors to consider.<sup>9</sup> In this view the preference for a flattened structure arises because conjugation with the aryl groups becomes possible when a  $D_2$  distortion occurs and the substituents twist toward the plane of the parent phenanthroline. The two types of interactions are not mutually exclusive and may, in fact, work hand in hand in shaping the structure. One last point worth noting is that  $\text{Cu}(\text{dpp})_2^+$  and  $\text{Cu}(\text{dptmp})_2^+$  exhibit emission at almost the same energy in dichloromethane solution despite having different excited-state geometries. An important part of the explanation is that neither system undergoes much structural relaxation in the excited state. For the  $\text{dptmp}$  complex a cooperative substituent effect mitigates the flattening distortion, while in the case of the  $\text{dpp}$  complex, intra- and/or interligand interactions predispose the ground state to adopt a flattened structure rather like that favored by the excited state.

**Summary**

Solid-state measurements establish that a flattening distortion has a large impact on the spectroscopic properties of a  $\text{Cu}(\text{NN})_2^+$  system, whereas a rocking distortion typically has little effect. If the dihedral angle between the two phenanthroline ligands (or its complementary angle) is in the range of 80–90°, the solid is orange or orange-red with a reflectance spectrum that exhibits an absorption band in the vicinity of 460 nm and a shoulder toward longer wavelength, consistent with approximate  $D_{2d}$  symmetry. In the other limit the dihedral angle is much smaller, the compound may even be purple, and the reflectance spectrum exhibits two bands, including intense absorption at 525 nm or beyond. In the ground state the flattening distortion is a solid-state effect, except for systems such as  $\text{Cu}(\text{dpp})_2^+$  and  $\text{Cu}(\text{dptmp})_2^+$ , which have phenyl substituents in the 2,9 positions of the phenanthroline ligand. However, the emissive excited state is subject to an intrinsic flattening distortion due to the Jahn–Teller active copper(II) character, though intra- or intermolecular forces can inhibit the effect. In particular, intramolecular steric interactions prevent a flattening distortion in the  $\text{Cu}(\text{dptmp})_2^+$  system because the 3,8 methyl groups restrict the conformational freedom of the neighboring phenyl groups. In the case of  $[\text{Cu}(\text{tmp})_2]\text{BPh}_4$ , packing interactions induce a small flattening in the crystal but oppose further distortion in the photoexcited state. Consequently,  $[\text{Cu}(\text{tmp})_2]\text{BPh}_4$  and, probably for the same reason,  $[\text{Cu}(\text{phen})_2]\text{BPh}_4$  are photoluminescent solids. This is the first report of emission from a bis(phenanthroline)copper(I) system that does not have bulky substituents in the 2 and/or 9 positions of the ligand.

## Summary

**Acknowledgment.** The National Science Foundation supported this research through Grant Number CHE-9726435.

**Supporting Information Available:** Four X-ray crystallographic files in CIF format. This material is available free of charge via the Internet at <http://pubs.acs.org>.

IC000082S

(29) Pearson, R. G. *Proc. Natl. Acad. Sci. U.S.A.* **1975**, *72*, 2104–2106.

(30) Turro, N. J. *Modern Molecular Photochemistry*; Benjamin/Cummings: Menlo Park, CA, 1978; pp 155–170.

(31) Kirchhoff, J. R.; Gamache, R. E., Jr.; Blaskie, M. W.; Del Paggio, A. A.; Lengel, R. K.; McMillin, D. R. *Inorg. Chem.* **1983**, *22*, 2380–2384.

(32) Dietrich-Buchecker, C. O.; Marnot, P. A.; Sauvage, J. P.; Kirchhoff, J. R.; McMillin, D. R. *J. Chem. Soc., Chem. Commun.* **1983**, 513–515.

(33) Miller, M. T.; Gantzel, P. K.; Karpishin, T. B. *Inorg. Chem.* **1999**, *38*, 3414–3422.

(34) Eggleston, M. K.; Fanwick, P. E.; Pallenberg, A. J.; McMillin, D. R. *Inorg. Chem.* **1997**, *36*, 4007–4010.

(35) Gushurst, A. K. I.; McMillin, D. R.; Dietrich-Buchecker, C. O.; Sauvage, J. P. *Inorg. Chem.* **1989**, *28*, 4070–4072.